DETERMINATION OF THE EFFECTIVE JET PUMPING SURFACE FOR CONICAL SEPARATED SUPERSONIC FLOW

By

Wayne John Young

Bachelor of Science

Taiwan Provincial Cheng-Kung University

Tainan, Taiwan, China

1955

Submitted to the faculty of the Graduate School of
the Oklahoma State University
in partial fulfillment of the requirements
for the degree of
MASTER OF SCIENCE
August, 1963

DETERMINATION OF THE EFFECTIVE JET PUMPING SURFACE

FOR CONICAL SEPARATED SUPERSONIC FLOW

Thesis Approved:

Thesis Advisor

Dean of the Graduate School

FOREWORD

The writer wishes to express his deep appreciation and gratitude to his academic advisor, Dr. G. W. Zumwalt, a gifted instructor and devoted educator, under whose direction this thesis is written. His over-all influence upon the writing of this thesis as well as throughout the writer's graduate career is beyond appraisal.

Also, grateful acknowledgments are extended to the members of the Mechanical Engineering Faculty whose capable instructions and warm encouragement are indelible to the writer.

The writer is also indebted to Mr. H. H. Tang, Dr. Zumwalt's assistant, for his guidance toward the accomplishment of this paper.

This paper is dedicated to the memory of the writer's mother, who did not live to see the graduation of her son.

TABLE OF CONTENTS

LIST OF FIGURES

LIST OF SYMBOLS

A		Area
A*		Critical flow area
B		Dimensionless group defined in Equation 2, page 8
C	=	u/u_{max}, Crocco number $= \left(\frac{M^2}{\frac{2}{k-1} + M^2}\right)^{\frac{1}{2}}$
erf		Error function, see page 4
f( )		Function of some variables
g_c		Dimensional conversion factor
G_d		Mass rate added to base region by each mixing stream, lb_m/sec
I_1		Integral associated with mass transport for plane flow as defined on page 8
I_2		Integral associated with momentum transport for plane flow as defined on page 8
J_1		Integral associated with mass transport for axi-symmetric flow as defined on page 8
J_2		Integral associated with momentum transport for axi-symmetric flow as defined on page 8
k		Ratio of specific heat
$\mathbb{K}$		Relation as defined on page 16
$\dot{m}$		Mass flow rate, lb_m/sec-sq ft
M		Mach number
p		Absolute pressure
r		Radius of mixing region
R		Radius of base
$\mathcal{R}$		Perfect gas constant
$\mathbb{R}$		A reference streamline near but outside the mixing region

T	Absolute temperature
u	Velocity in x or X direction
x,y	Coordinates of the intrinsic coordinate system
X,Y	Coordinates of the reference coordinate system
β	Variable in error function
σ	Similarity parameter of the homogeneous coordinate y/x (also called the free jet spreading parameter)
η	$= \sigma \frac{y}{x}$, Dimensionless coordinate
θ	Streamline angle
ρ	Density
φ	$= u/u_a$, Dimensionless velocity
ν	Prandtl-Meyer turning angle

Subscripts:

1,2,3,4	Refer to conditions at cross sections indicated in Figure 1
a	Refers to conditions of the flow in the isentropic stream adjacent to the dissipative regions
b	Refers to the conditions at the base of the sudden expansion
d	Refers to the streamline whose kinetic energy is just sufficient to enter the recompression region
j	Refers to conditions along the jet boundary streamline
m	Refers to coordinate shift in the mixing theory due to the momentum integral
o	Stagnation conditions
R	Refers to conditions along R streamline
∞	Refers to upstream condition

CHAPTER I

INTRODUCTION

The determination of base pressure under highly transient conditions is a rather complex problem, due to the lack of any adequate theory for predicting this pressure for axi-symmetric bodies even at steady condition (1, 2, and 3). A useful approach to this problem has been made first by Korst (4) in 1954 for two-dimensional bodies under steady state assumptions. Further a conical wake analysis was attempted to extend two-dimensional theory to axially symmetric cases under steady flow conditions by Zumwalt (2).

No method is available to predict base pressure with mass transfer in the base region for an axi-symmetric body, such as occurs when a blast wave passes a flying vehicle. It is the purpose of this paper to compare the recent analysis developed by Zumwalt and his associates with experiments performed by Sandia Corporation personnel.

Within the scope of this paper mass addition at the base will be used to simulate the actual blast wave transient effect on axi-symmetric base pressure and quasi-steady state will be assumed for the actual highly transient problem.

A brief review of the theoretical background will now be given in Chapters II and III. The test program will be described in Chapter IV and a comparison made in Chapter V.

CHAPTER II

THEORETICAL BACKGROUND

A. Two Dimenstional Constant Pressure Turbulent Jet Mixing

The following assumptions have been made in Korst's theory of turbulent jet mixing (4):

1. two-dimensional backstep
2. tubulent flow in the mixing region
3. constant pressure isoenergetic jet mixing
4. the boundary layer is very thin compared to the jet mixing length.

Characteristic features of the flow model are:

1. Prandtl-Meyer expansion at separation corner
2. Recompression pressure is defined by an oblique shock in the free stream.
3. Boundary layer at separation is turbulent, fully developed and the base pressure is dependent of Reynolds number of free stream.

The flow model used is shown in Figure 1.

Of particular interest are the streamline, j, which is separated from the corner of the base, and the streamline, d, along which the particles just have enough kinetic energy to reach the recompression region. Particles below the line d will recirculate inside the dead

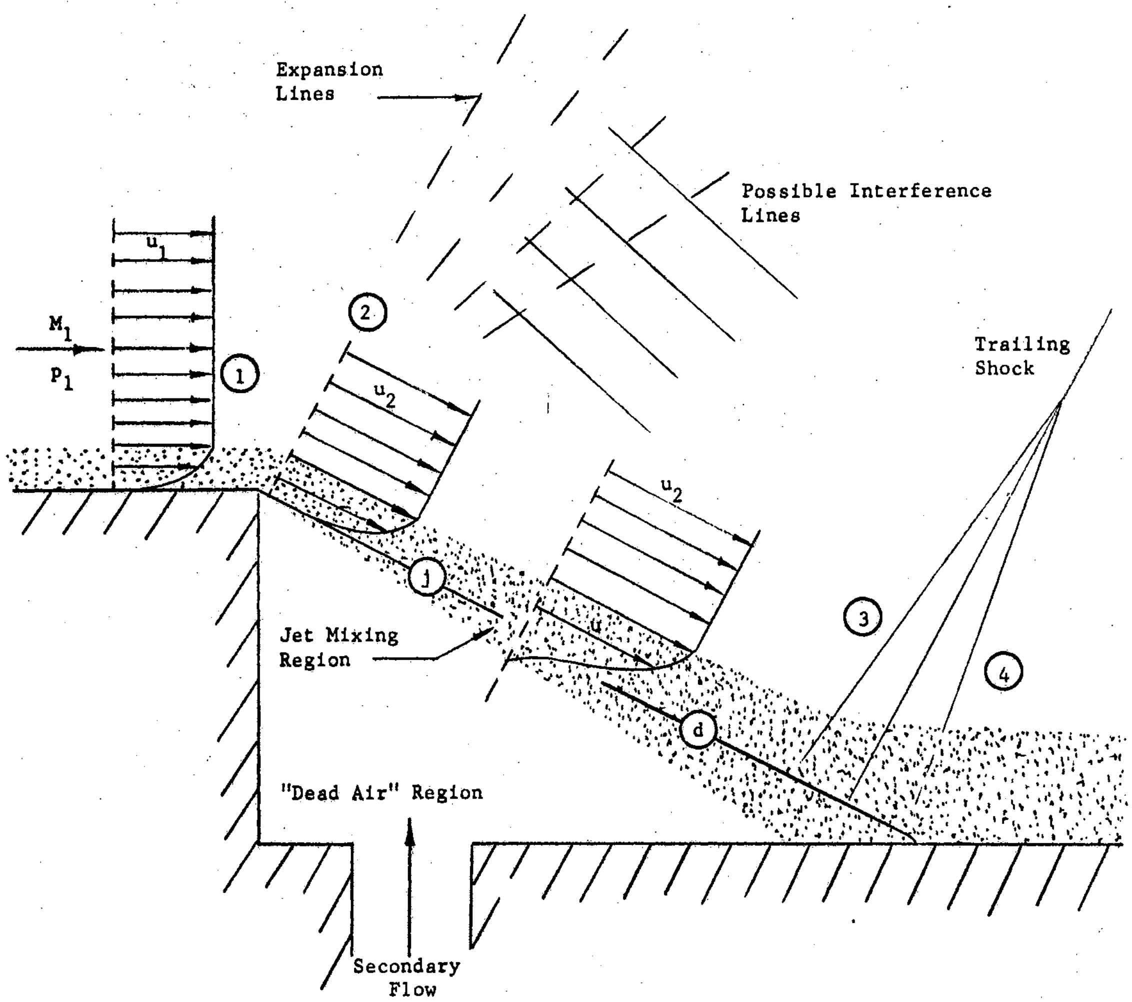

Figure 1. Model for the Constant Pressure Jet Mixing Analysis

air region. Streamlines j and d are identical if there is no mass fed into wake, i.e. steady state condition. In case of mass bleed-in, the streamline j will have higher velocity than streamline d and vice versa for mass bleed-out. From no-bleed, base pressure can be calculated without using any empirical information.

In deriving the theory, Korst applied the equation of motion along an intrinsic system of coordinates which was located in space by its displacement from a corresponding inviscid jet boundary. With this transformation, an asymptotically approached velocity profile was found as

$$\phi = \frac{u}{u_2} = \tfrac{1}{2}(1 + \operatorname{erf}\eta) \qquad \text{(Eq. 1)}$$

This is the velocity profile in a two-dimensional, constant pressure, fully developed, turbulent, isoenergetic, jet mixing region. Here, u denotes the x-component of velocity in the mixing region, u_2 denotes the x-component fo free stream velocity adjacent to the mixing region, and η is a position parameter for the direction normal to the flow, $\eta = \sigma y/x$. x,y are intrinsic coordinates with $y = 0$ at $u = \tfrac{1}{2}u_2$, and $x = 0$ at the separation corner. y is displaced from the inviscid jet boundary coordinate Y. σ is the jet spreading parameter, depending on the free stream Mach Number, M_2, or on $C_2 = u_2/u_{2max}$, and

$$\operatorname{erf}\eta \equiv \frac{2}{\sqrt{\pi}} \int_0^{\eta} e^{-\beta^2} d\beta$$

This asymptotic solution can be used to calculate the kinetic energy level among the streamlines in the mixing region.

B. Conical Wake Analysis

Referring to Figure 2 of flow model, because of complicated interference waves due to the three dimensionality of the flow, a coalescing trailing shock would vary in strength with the distance from the test body. Close to the test body surface it is approximately two dimensional in charater, but it becomes nearly conical at sufficiently large distance. Owing to the complexity of theoretical approach, an approximate method has been developed by Zumwalt (2).

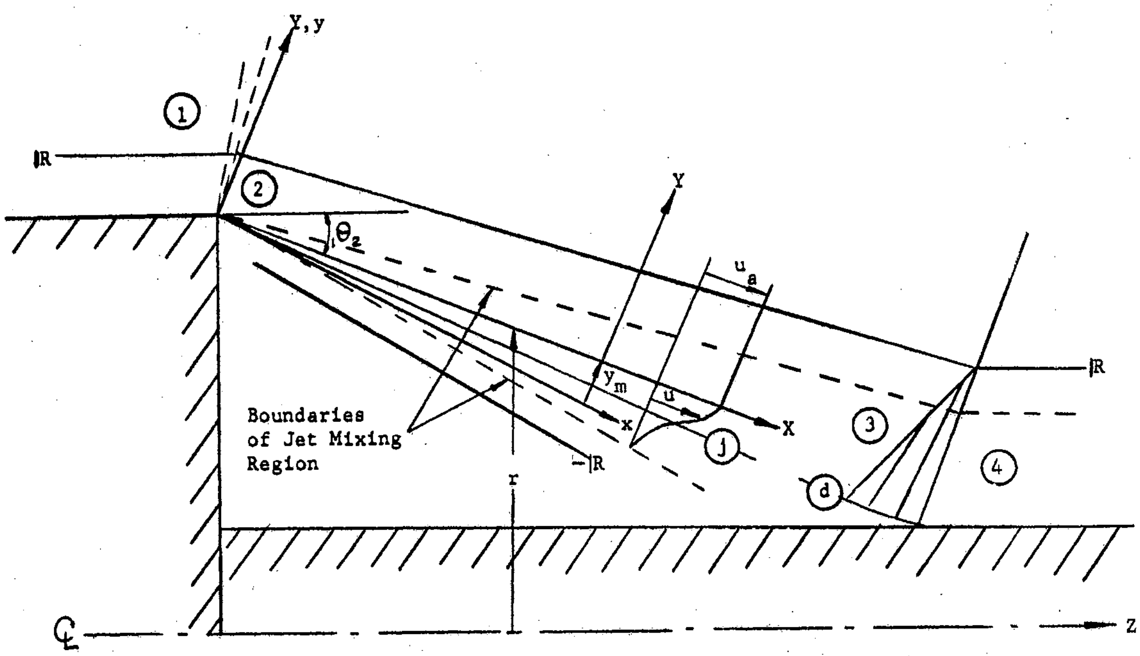

Figure 2. Flow Model for Use in the Analysis of a Free Jet Boundary with Rising Pressure

Zumwalt, basing on Korst's two dimensional mixing theory, attempted to solve the axi-symmetric base pressure problems with two separate treatments, one for internal expanding jets and the other for external jet boundaries. The former one will not be introduced here as it is not applicable to this paper.

For external flow past axi-symmetric bodies with suddenly reduced diameter the following conclusions have been reached:

1. The use of two-dimensional expansion at the separation corner is acceptable unless boundary thickness is appreciable.

2. The assumption of constant pressure mixing becomes invalid, as may be seen from results obtained by using this assumption in Figure 3. Instead, a new assumption of potential flow past a cone is utilized for defining the pressure field in the mixing region. This can be substantiated with Schlieren pictures and measurement of E. S. Love (5).

3. The cone, as utilized in 2 above, also serves as the corresponding inviscid jet boundary. Since a pressure gradient exists along the streamlines, further modification of the flow can be expected.

4. The using of the error function velocity profile has been proved to be advantageous.

5. Radius effects on the jet coordinate location are appreciable and were determined by analytical means.

6. The oblique shock recompression was used in calculations. Satisfactory agreements with experimental data on test bodies with cylindrical extensions are found and remarkable improvements over the previous attempts of applying two-dimensional theory directly are shown (see Figure 2).

To analyze the jet mixing region with pressure rise, in addition to defining the coordinate systems in the same way as Korst, Zumwalt added two more assumptions.

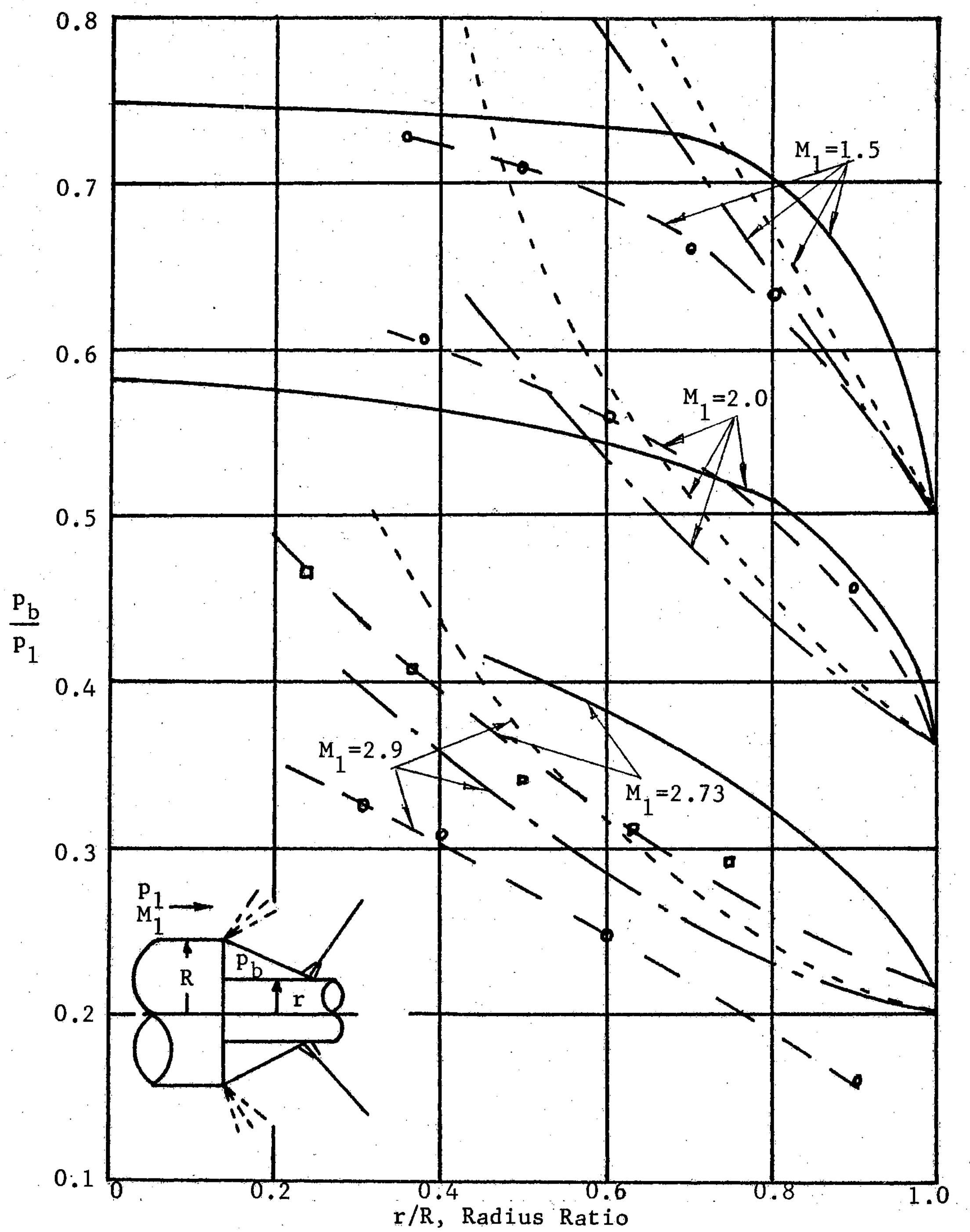

— ⊖ — —	Experiment, Ref. 14
— — ⊟ —	Experiment, Ref. 15
——— - ———	Constant Pressure Mixing, Ref. 2
————————	Conical Pressure Rise Theory, Ref. 2
— — — — — —	Korst's Two-Dim. Solution Adapted to Axial-Symmetry

Figure 3. Comparison of the Conical Flow Theory with Experiment for External Flow Past a Cylinder with Reduced Radius

1. The pressure gradient normal to the "corresponding inviscid jet boundary" is zero in the vicinity of and within the mixing region, while the pressure change along the region is the same as that along a conical surface coinciding with the "corresponding inviscid jet boundary."

2. The velocity of the jet adjacent to the region is that which would prevail along the conical corresponding inviscid jet boundary.

He applied momentum equation in the axial direction with some geometrical and reference coordinate transformation and solved simultaneously with the combined viscid and inviscid continuity equation between the cross section of separation corner 2 and a downstream cross section 3, for the mass passing along the annular stream tube bounded by streamline j and a large value of η_{IR} (= 3), where subscript IR refers to the streamline far away from the mixing region, i.e. undisturbed region.

Finally, a governing equation is obtained as follows:

$$(B-3)^2 + 2(1-C_{3a}^2)\left[I_1\Big|_{-\infty}^{3} - I_1\Big|_{-\infty}^{\phi_j} \right] B - 2(1-C_{3a}^2)\left[J_1\Big|_{-\infty}^{3} - J_1\Big|_{-\infty}^{\phi_j} \right] = \left[\frac{\sigma r}{x\cos\theta} \right]_3^2$$

$$B = \frac{J_1\Big|_{-\infty}^{\phi_j} - \left(1-\frac{C_{3a}}{C_{2a}}\right) J_1\Big|_{-\infty}^{3} - \frac{C_{3a}}{C_{2a}}(J_1 - J_2)\Big|_{-\infty}^{3}}{I_1\Big|_{-\infty}^{\phi_j} - \left(1-\frac{C_{3a}}{C_{2a}}\right) I_1\Big|_{-\infty}^{3} - \frac{C_{3a}}{C_{2a}}(I_1 - I_2)\Big|_{-\infty}^{3} + \frac{k-1}{k}\frac{3}{C_{2a}C_{3a}}\left(1-\frac{P_2}{P_3}\right)} \quad \text{(Eq. 2)}$$

where

$$I_1 = \int_{-\infty}^{\eta} \frac{\varphi}{1 - C_{2a}^2\varphi^2}\, d\eta$$

$$I_2 = \int_{-\infty}^{\eta} \frac{\varphi^2}{1 - C_{2a}^2\varphi^2}\, d\eta$$

$$J_1 = \int_{-\infty}^{\eta} \frac{\varphi\eta}{1 - C_{2a}^2\varphi^2}\, d\eta$$

$$J_2 = \int_{-\infty}^{\eta} \frac{\varphi^2\eta}{1 - C_{2a}^2\varphi^2}\, d\eta$$

and these integrals are functions of C_{3a}^2 and the working curves of these are shown in Zumwalt Ph.D. dissertation (2).

The subscript "a" denotes flow adjacent to the mixing region in the base with pressure rise condition. Noting that r is the radius of the mixing region in the above equation and if r approaches infinity, the solution will reduce to the two-dimensional case.

In short, Zumwalt's conical flow analysis rests on a fairly solid foundation as the model used nearly conforms to reality and analysis stems from basic flow laws and mixing theory rather than being simply a data correlation technique, as is done in other recent axi-symmetric methods (3).

Unfortunately, however, this method is lengthy and tedious due to the complexity of the above stated equation and the need for several integral function curves. Furthermore, a set of solutions of flow past conical boat tails is required to furnish the information for the inviscid jet boundary flow conditions. That is, values of P_2/P_3 and C_{3a}/C_{2a} on conetails are required for various radius r and cone angles θ for different approaching Mach numbers or Crocco numbers. To eliminate this latter requirement, an empirical equation (6) has been obtained:

$$M_{3a} = \frac{M_{2a}}{e^{0.209(1-r/R)}} \qquad \text{(Eq. 3)}$$

where M_{2a} denotes Mach number after Prandtl Meyer expansion and M_{3a} denotes the Mach number before the oblique shock recompression.

All axi-symmetric flow field theory becomes invalid on the center line where flows converge and axi-symmetric base pressure theory behaves likewise. The mathematical difficulties occurred in treating the flow field of an axisymmetric body with abruptly reduced base can be readily solved by using an imaginary concentric cylindrical extension shown in Figure 2. In developing conical pressure theory for this new flow model, fortunately, it was found that base pressure remained almost constant when the radius ratio r/R becomes smaller than 0.4 and this prediction satisfactorily agrees with experiment (3). Therefore, the theory which assume a small concentric cylindrical extension on the base is sufficiently accurate to be used to determine the base pressure of an axi-symmetric blunt body.

This conical pressure rise theory for separated flows has been utilized to calculate the axi-symmetric body base pressure (6).

In order to check the theory with some published experimental data, some typical solutions for steady state flow have been calculated for $M_1 = 1.5$, 2.0, 4.0 and 5.0. From the results of calculation, curves of pressure ratio P_b/P_1 versus radius ratio r/R have been plotted with Mach number as parameter. This is shown in Figure 4.

C. Base Pressure with Mass Addition into the Wake

1. Basic Description

Duplication of blast waves of the magnitude of those produced by nuclear blasts is impossible without actual atmospheric explosions. Therefore, in the prediction of blast wave effect on missile base pressure we use mass bleeding from the base into the wake to substitute for the effects which are produced by the actual explosions. This leads to the establishing of the interactions between mass addition into the wake and base pressure variations, and for an approximate analysis, it is treated under a quasi-steady condition. In blast wave interactions, as a matter of fact, it is a highly transient problem.

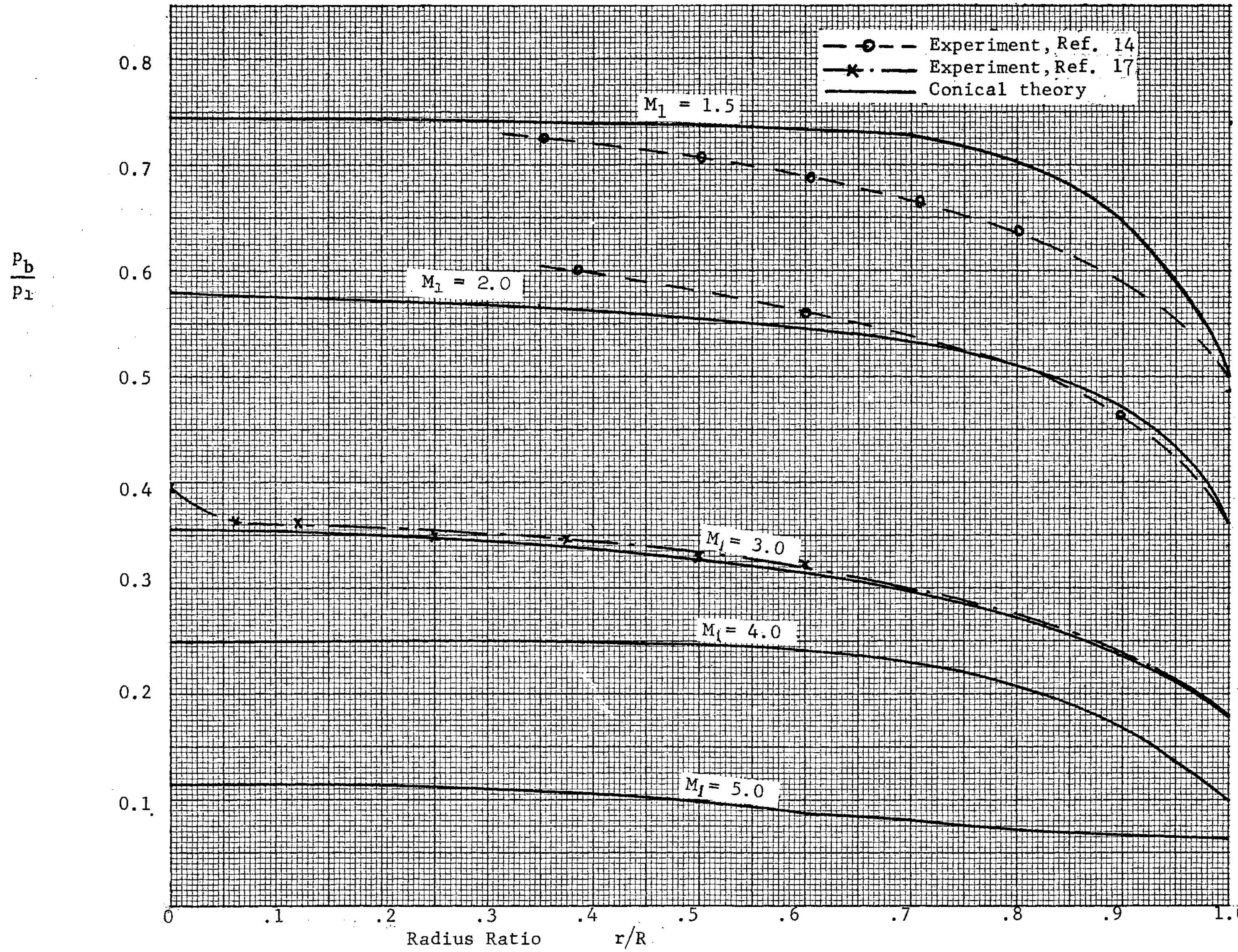

Figure. 4 Comparison of the Conical Flow Theory with Experiment for External Flow Past a Cylinder with Reduced Radius.

To consider the blast wave effect on base pressure, we note the wave, which is a normal shock, passing the body with transient conditions following the shock, i.e. pressure varies after the passing of wave. In this flow of transient nature, a certain amount of mass will flow into or out of the wake or dead air region to adjust the base pressure to tend toward a steady state or stable condition. Thus, it can be readily seen that part of the conical surface has an ejecting effect during the period after the blast wave passage.

The change in pressure due to mass exchange may be augmented or opposed by the gradually decreasing pressure in the ambient stream. Thus the base pressure does not stay unchanged, due to the difference between the stable value in equilibrium condition and the value instantaneously in the transient pressure field.

It was desired to obtain values of the effective radius ratio, r/R, for jet pumping action of the mixing ration. These values were expected to depend on M_1 and on the rate of mass addition. The later can be expressed as a dimensionless bleed rate $\mathcal{H}$, defined as:

$$\mathcal{H} = \frac{G_d\sqrt{T_o}}{P_o A_b}\sqrt{\frac{R}{g_c k}}$$

substituting

$$R = 53.3 \text{ ft-lb}_f/\text{lb}_m\text{-}^{\circ}\text{R}$$

$$g_c = 32.2 \text{ lb}_m\text{ft/sec}^2\text{lb}_f$$

$$k = 1.4$$

yields

$$\mathcal{H} = 1.088 \frac{G_d\sqrt{T_o}}{p_o A_b} \qquad \text{(Eq. 4)}$$

For calculating base pressures, an experimental jet spreading parameter, σ, is required and is suggested by Tripp (7) as

$$\sigma = 12 + 2.758\, M_{2a}$$

where M_{2a} denotes the Mach number of the free stream adjacent to the jet mixing region. It has been shown by Maydew and Reed (8), and by Zumwalt and Chrisman (9) that this linear relation has underestimated σ values for higher supersonic flows. An tentative empirical equation has been suggested by Zumwalt and Tang (10) as

$$\sigma = 47.1\, Cr^2 \qquad \text{(Eq. 5)}$$

for $1.22 < M_2^2 < 5$.

2. Mass Transfer of a Conical Wake

To derive an expression for mass addition rate G_d, Tang (11) has superimposed Korst's mixing theory and Zumwalt's conical wake analysis with additional consideration of conservation of mass. His approach can be described briefly as follows:

The mass flow rate between streamline η_j and η_d can be expressed in differential form as

$$d\dot{m} = d(\rho u A)$$

Integrating this from Y_j to Y_d, it is seen that if mass is fed into the wake through the mixing region, streamline j has a lower velocity than streamline d and vice versa for the bleeding-out case, Figure 5, yields the mass addition rate,

$$G_d = \int_{Y_j}^{Y_d} \rho u 2\pi R\, dY$$

where

$$R = r + Y \cos\theta \qquad \text{and}$$

$$dY = dR/\cos\theta$$

Using $$\eta = \sigma \frac{Y}{x}$$

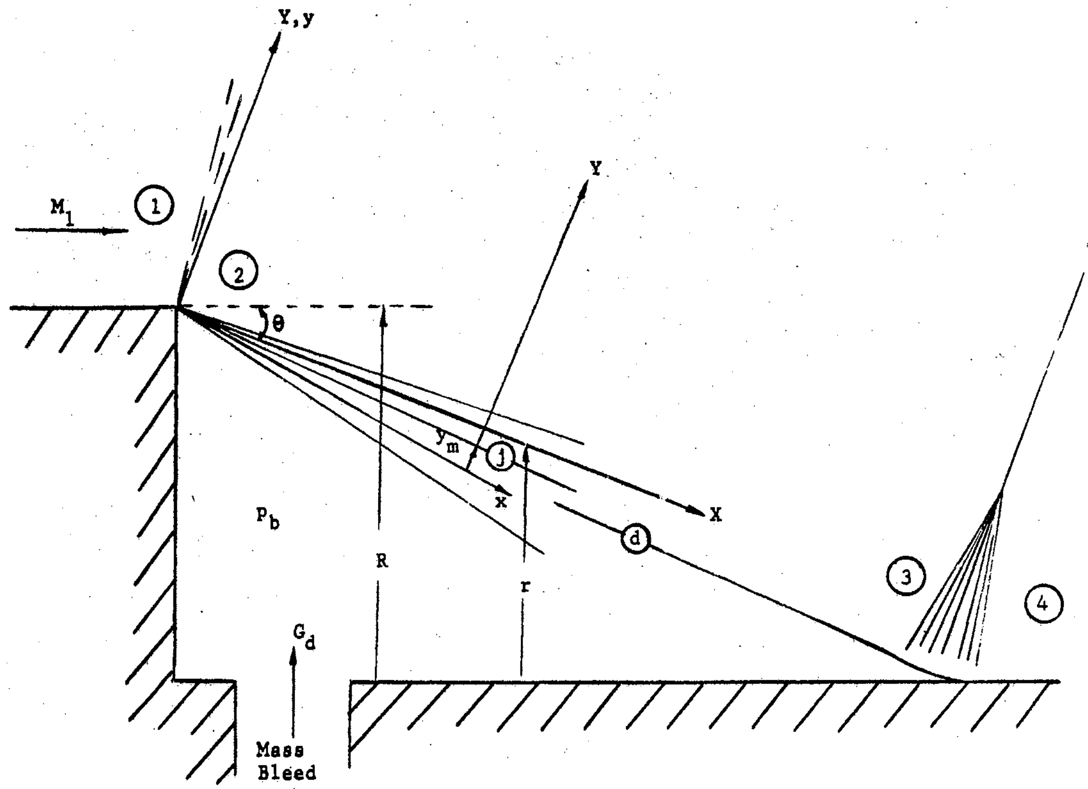

Figure 5. Mass Added to the Wake

and introducing dimensionless shift y_m of actual coordinates (x,y) from the coordinates for an inviscid jet (X,Y), (13), to get intrinsic coordinates x,y, the above expression is transformed as,

$$G_{T_d} = 2\pi \int_{\eta_j}^{\eta_d} \rho u \left[r + \frac{x}{\sigma} (\eta - \eta_m) \cos\theta \right] \frac{x}{\sigma} d\eta$$

$$= 2\pi \rho_{3a} u_{3a} \int_{\eta_j}^{\eta_d} \frac{\rho}{\rho_{3a}} \frac{u}{u_{3a}} \left[r + \frac{x}{\sigma} (\eta - \eta_m) \cos\theta \right] \frac{x}{\sigma} d\eta$$

For constant pressure across mixing region,

$$\frac{\rho}{\rho_{3a}} = \frac{T_{3a}}{T} = \frac{1 - C_{3a}^2}{1 - C_{3a}^2 \varphi^2} \qquad \text{and } \varphi = \frac{u}{u_{3a}}$$

Solving for η_m by the momentum equation in a form similar to that just written for the continuity equation, η_m can be eliminated. This result is,

$$G_d = 2\pi \left(\frac{x}{\sigma}\right)^2 \rho_{3a} u_{3a} (1 - C_{3a}^2) \cos\theta \left[(J_{1d} - J_{1j}) - B(I_{1d} - I_{1j}) \right]$$

where:

$$I_1 = \int_{-\infty}^{\eta} \frac{\varphi}{1 - C_{2a}^2 \varphi^2} d\eta$$

$$J_1 = \int_{-\infty}^{\eta} \frac{\varphi \eta}{1 - C_{2a}^2 \varphi^2} d\eta$$

$$B = \frac{J_1 \Big|_{-\infty}^{\varphi_j} - \left(1 - \frac{C_{3a}}{C_{2a}}\right) J_1 \Big|_{-\infty}^{3} - \frac{C_{3a}}{C_{2a}} (J_1 - J_2) \Big|_{-\infty}^{3}}{I_1 \Big|_{-\infty}^{\varphi_j} - \left(1 - \frac{C_{3a}}{C_{2a}}\right) I_1 \Big|_{-\infty}^{3} - \frac{C_{3a}}{C_{2a}} (I_1 - I_2) \Big|_{-\infty}^{3} + \frac{k-1}{k} \frac{3}{C_{2a} C_{3a}} \left(1 - \frac{P_2}{P_3}\right)}$$

Noting that;

$$\rho_{3a} u_{3a} = \sqrt{\frac{k g_c}{R}} \frac{P_0}{\sqrt{T_0}} \frac{P_{3a}}{P_0} \sqrt{\frac{T_0}{T_{3a}}} M_{3a} \qquad \text{and using}$$

isentropic relationships and the definition of Mach number;

$$\frac{P_{3a}}{P_0} = \left(1 + \frac{k-1}{2} M_{3a}^2\right)^{-\frac{k}{k-1}}$$

$$\sqrt{\frac{T_0}{T_{3a}}} = \left(1 + \frac{k-1}{2} M_{3a}^2\right)^{\frac{1}{2}}$$

$$x_{3a} = \frac{R - r}{\sin\theta} \Big|_{3a}$$

Finally, we obtain the form

$$G_d = \frac{P_0}{\sqrt{T_0}} \left[\frac{1}{\sigma_3} \frac{\cot\theta}{\sin\theta} K \right] \left[(J_{1d} - J_{1j}) - B(I_{1d} - I_{1j}) \right] \left(1 - \frac{r}{R}\right)^2$$

where:

$$\mathbb{K} = \frac{8\left(\frac{2}{k+1}\right)^{\frac{k+1}{2(k-1)}}\left(1 - C_{3a}^{2}\right)}{\frac{A_{3a}}{A^{*}}\sqrt{\frac{R}{g_c k}}} \qquad \text{(Eq. 7)}$$

and it is determined by M_{3a} and properties of the flowing gas.

CHAPTER III

CALCULATION OF EFFECTIVE JET PUMPING SURFACE WITH MASS ADDITION INTO THE WAKE

The aim of this calculation is to evaluate the relation between radius ratio r/R and dimensionless mass bleeding rate $\mathcal{H}$. This will be done by use of a relation between p_b/p_1 and $\mathcal{H}$ which can be found from the result of the Sandia Corporation experiments. In the following calculation and tests, $M_1 = 2$ is used, and the corresponding Prandtl-Meyer turning angle, ν, is 26.38^o and pressure ratio p_1/p_o is 0.1278. The following steps shows the calculation procedure.

A. For any value of p_b/p_1, noting that $p_b/p_1 = p_2/p_1$, we randomly select a value of r/R. This represents the radius at which the pumping action of the jet mixing surface ceases.

B. From value of p_b/p_1, the following values can be calculated or determined in sequence:

1. $p_2/p_{o_2} = (p_1/p_{o_1}) \times (p_2/p_1)$, since $p_{o_1} = p_{o_2}$
2. M_{2a} can be found by knowing p_2/p_{o_2}, also
3. ν_2
4. $C_{2a} = \sqrt{M_{2a}^2/(5 + M_{2a}^2)}$
5. $\theta = \nu_2 - \nu_1$
6. $\cot\theta$ / $\sin\theta$ and $\tan\theta$

C. Calculate M_{3a} by the relation

$$M_{3a} = \frac{M_{2a}}{e^{0.209(1 - r/R)}}, \quad C_{3a} = \sqrt{\frac{M_{3a}^2}{5 + M_{3a}^2}} \qquad \text{and}$$

spreading parameter σ_{3a} by the relation

$$\sigma_{3a} = 47.1 \times C_{3a}^2$$

D. Calculate or determine the following items:

1. $\mathbb{K}$ by Eq. 7

2. ϕ_j through C_3/C_2, C_3^2, and $\left[\sigma_3 \tan\theta\right]^2 / \left[\frac{1}{r/R} - 1\right]^2$ from computation curves (6).

3. B by Eq. 2 or computation curves (6).

E.

1. Calculate C_d by

$$C_d^2 = \left[1 - \frac{1}{(p_4/p_3)^{0.286}}\right] \tag{13}$$

2. Calculate ϕ_d by

$$\phi_d = C_d/C_{3a}$$

3. Determine the values of J_{1d} and I_{1d} through C_{3a}^2 and ϕ_d from Reference (2).

F. Substitute the above related items into

$$\mathcal{H} = 1.088 \frac{G_d\sqrt{T_0}}{P_0 A_b} = \frac{1.088}{\sigma_{3a}^2} \frac{\cot\theta}{\sin\theta}\left(1 - \frac{r}{R}\right)^2 \left[(J_{1d} - J_{1j}) - B(I_{1d} - J_{1j})\right]$$

By adjusting r/R value, a trial and error method is used to obtain a proper r/R which yields the same $\mathcal{H}$ as obtained by experiment for the same base pressure ratio, p_b/p_1.

G. By repeating the same procedure we can construct a curve showing the relation between r/R and $\mathcal{H}$, as well as p_b/p_1, for a given M_1.

CHAPTER IV

ANALYSIS OF EXPERIMENTAL DATA

A. Experimental Equipment

To evaluate experimentally the effective jet pumping surface, personnel at Oklahoma State University designed a test device and requested Sandia Corporation to construct this and conduct a test program (13).

The facilities developed by Sandia Corporation for this experiment consists of:

1. A nozzle plenum chamber which contains a 685.6 cu. in. (inside volume) concentic inner chamber.

2. A Mach 2.0 annular nozzle in which is mounted a 2.123 in O.D. tube, extending from the inner chamber, that simulates a circular body of revolution having a flat base.

3. A diffuser to enable the nozzle to operate at Mach 2.0 using lower stagnation pressures, and thereby gaining longer running times from a stored air supply.

Related facilities were developed to provide several flow rates through the center tube. A metering nozzle connected to the inner chamber could be opened to a vacuum source or to atmospheric pressure. The equipment and test installation are shown in Figure (6).

B. Experimental Program

The experimental program was divided into two phases: calibration

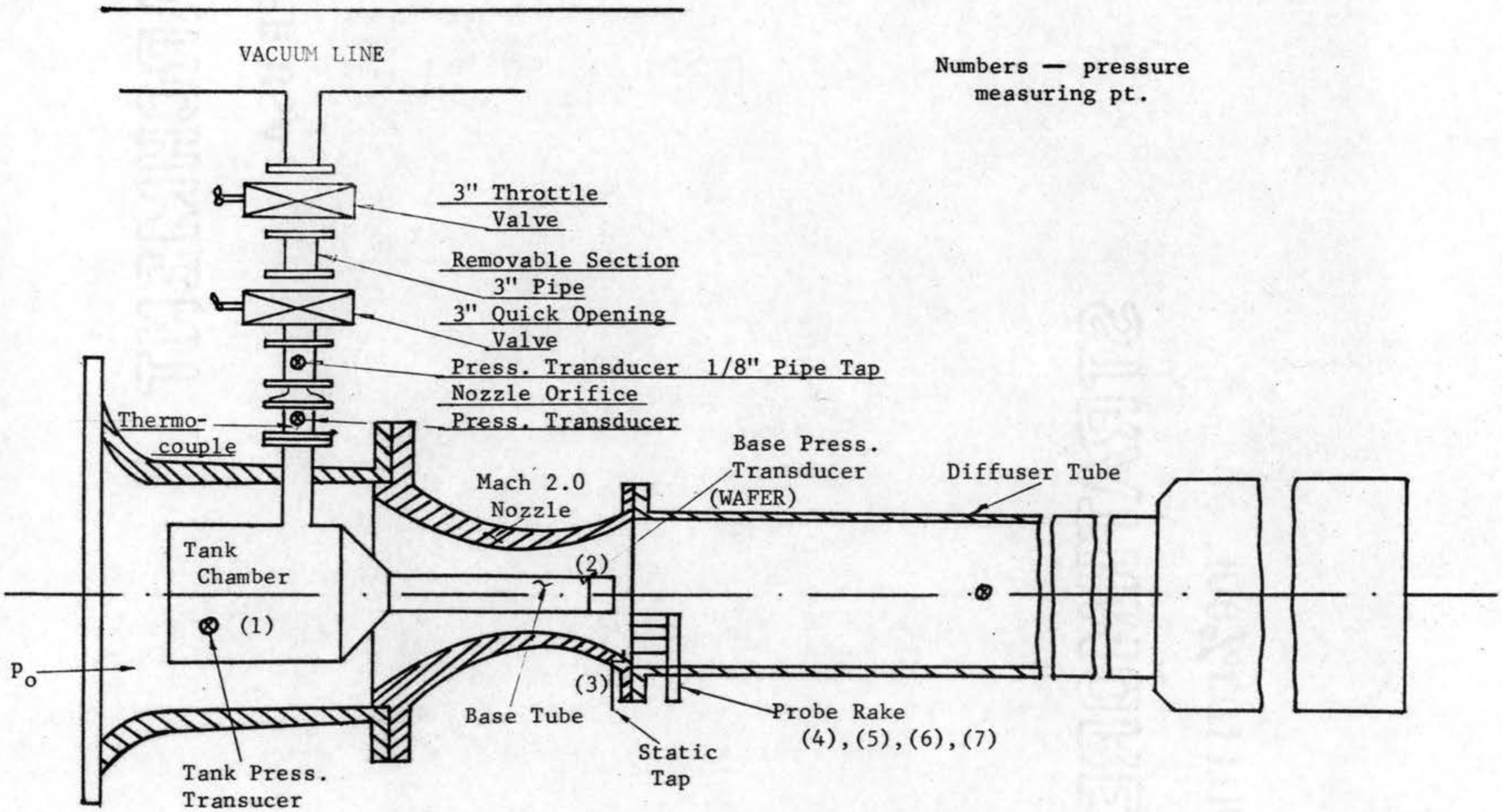

Figure 6. Experimental Equipment

and steady state. Phase 1 was to calibrate the Mach 2.0 nozzle with the center tube. A static pressure port at the nozzle exit, and a rake with 4 total head probes were used to determine Mach number and Mach distribution.

Base pressure was measured by a pressure transducer located in the inner tank chamber.

Phase 2 was to determine the effect on base pressure when metered flows are bled into or out of the center tube.

1. Bleed-in: the tank chamber is vented to a vacuum source through a metering nozzle type orifice. Three orifices were selected with diameters of 0.625, 0.875 and 1.5 inches to allow mass flows through the center tube of approximately 0.0184, 0.0249 and 0.0318 lb_m/sec respectively.

2. Bleed-out: the tank chamber is vented to ambient pressure (approximately 12.06 psia) through similar type metering nozzles. The orifice diameters selected for this part are: 0.625, 0.875, 1.000, and 1.125 inches to allow mass flows out of the center tube of approximately 0.083, 0.1634, 0.2171, and 0.2735 lb_m/sec respectively.

The flow rates were computed assuming sonic flow through the orifices with no losses throughout the system:

$$\dot{m} = A^* \sqrt{\left(\frac{2k g_c}{k-1}\right)\left(\frac{P_1}{v_1}\right)\left[\left(\frac{P_2}{P_1}\right)^{\frac{2}{k}} - \left(\frac{P_2}{P_1}\right)^{\frac{k+1}{k}}\right]} \qquad (12)$$

where

$k = 1.4$

$g_c = 32.2 \ lb_m ft/sec^2 lb_f$

$R = 53.3 \ ft\text{-}lb_f/lb_m\text{-}^{\circ}R$

which reduces to

$$\dot{m} = 0.532 \frac{A^* p_o}{\sqrt{T_o}} \qquad lb_m/sec$$

A typical phase 2 test run consisted of establishing Mach 2.0 flow past the center tube exit, and then opening a quick-acting valve to allow flow in or flow out of the center tube. When tank chamber pressure and base pressure reached equilibrium, data were taken. Base pressure was determined from a wafer gage (pressure transducer) located just inside the center tube exit.

Test data from the two phases were recorded on IBM punch cards and tabulated.

C. Data Analysis

1. Calibration Test

(Samples are chosen randomly from 15 runs.)

Run No.		1	2	15
P_{ox}		49.89	39.66	49.73
At	p_3	6.23	4.892	6.562
Position	p_3/p_{ox}	0.1249	0.1233	0.132
3	M_3	2.014	2.023	1.985
At	P_{oy4}	35.59	28.34	35.79
Position	P_{oy_5}/P_{ox}	0.7134	0.7145	0.7197
4	M_4	2.016	2.014	2.002
At	P_{oy_5}	35.56	28.32	35.67
Position	P_{oy_5}/P_{ox}	0.7128	0.7141	0.7173
5	M_5	2.017	2.015	2.008
At	P_{oy_6}	35.79	28.49	35.91
Position	P_{oy_6}/P_{ox}	0.7175	0.7184	0.7221
6	M_6	2.007	2.005	1.997
At	P_{oy_7}	35.90	28.50	35.83
Position	P_{oy_7}/P_{ox}	0.7190	0.7186	0.7205
7	M_7	2.014	2.023	1.985

The average Mach No. is 2.003 and the corresponding p/p_o is 0.127. The positions are shown in Figure 6.

2. Steady Bleeding Tests.

	Vented to Atmosphere				Vented to Vacuum		
Run No.	20	21	22	23	24	25	26
Orifice Dia. (in.)	0.625	0.875	1.000	1.125	0.625	0.875	1.5
A^* (sq. in.)	0.3066	0.6010	0.7850	0.9935	0.3066	0.6010	1.7660
$\sqrt{T_o}$ $(^oR)^{\frac{1}{2}}$	23.7	23.6	23.2	23.1	23.05	23.10	23.10
p_o (psia)	12.06	12.06	12.06	12.03	2.60	1.803	0.782
$\dot{m} = 0.532 \frac{A^* p_o}{\sqrt{T_o}} \left(\frac{lb_m}{sec}\right)$	0.0830	0.1634	0.2171	0.2753	-0.0184	-0.0249	-0.0318
A_b (sq. in.)	3.538	3.538	3.538	3.538	3.538	3.538	3.538
p_{oa} (psia)	50.15	49.77	50.12	50.10	50.07	50.13	50.12
$\mathcal{H} = \frac{\dot{m}\sqrt{T_o}}{P_o A_b}\sqrt{\frac{R}{g_c k}}$	0.0121	0.0238	0.0309	0.0391	-0.0026	-0.0035	-0.0045
p_b (psia)	5.227	6.132	6.418	6.939	2.600	1.802	0.782
$\bar{p}_1$ (psia)	6.369	6.321	6.365	6.363	6.359	6.397	6.365
$p_b/\bar{p}_1$	0.787	0.909	0.941	1.005	0.388	0.266	0.104
Calculated r/R (from Fig. 8)	0.82	0.90	0.09	0.90	0.385	0.27	0.20

Results of p_b/p_1 and r/R versus $\mathcal{H}$ are plotted in Figure 7.

The average of no-bleed data yields $p_b/p_1 = 0.565$, while Zumwalt's theoretical solution is 0.58 (6).

The calculated results of mass bleed rate versus effective pumping radius ratio are plotted in Figure 8. An equation can be written approximating the linear section of the curve:

$$r/R = 0.55 + 77.5\,\mathcal{H} \qquad \text{(Eq. 8)}$$

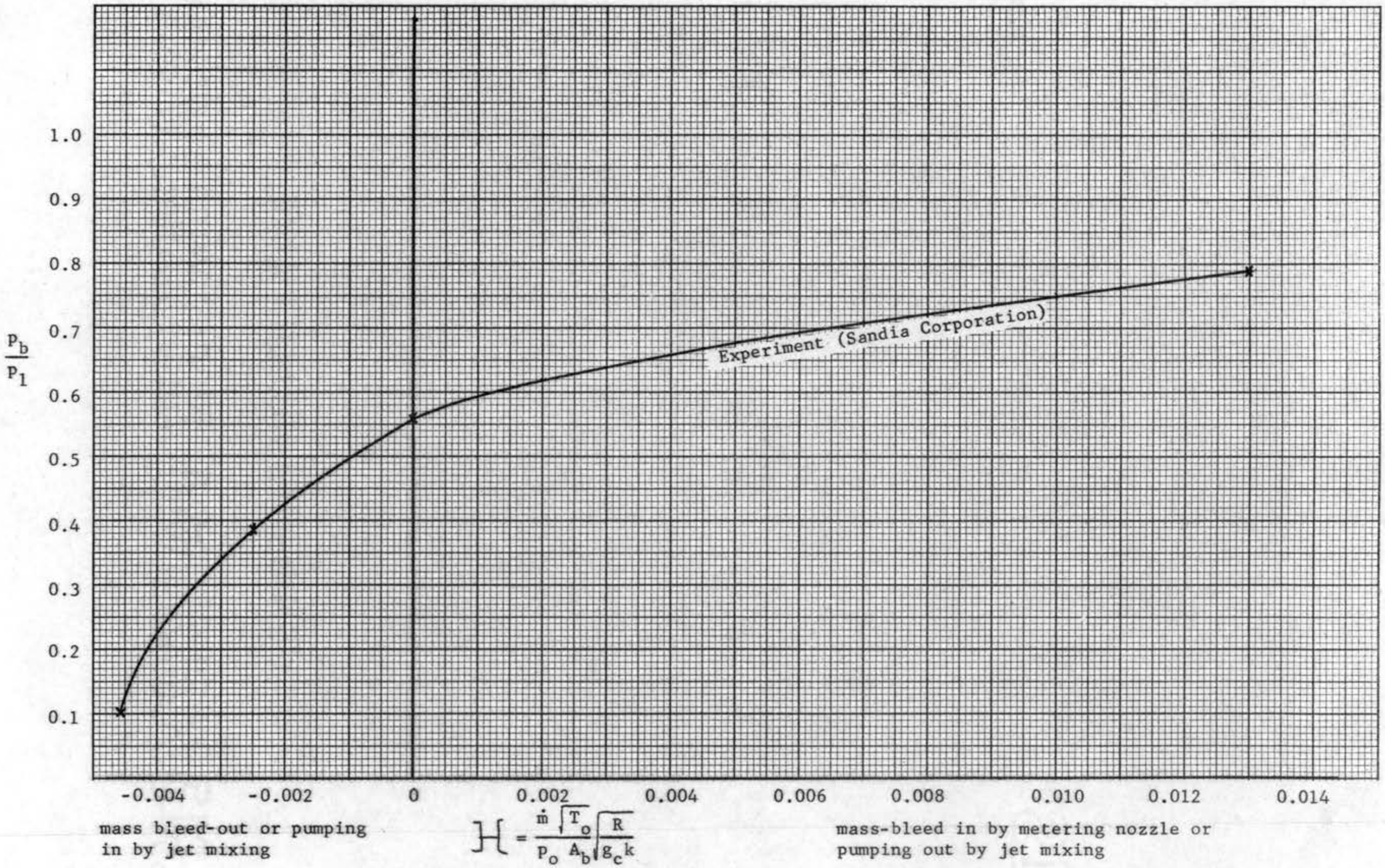

Figure 7. Dimensionless Mass Bleeding Rate versus Pressure Ratio for $M_1 = 2$. Result of Experiment Performed by Sandia Corporation.

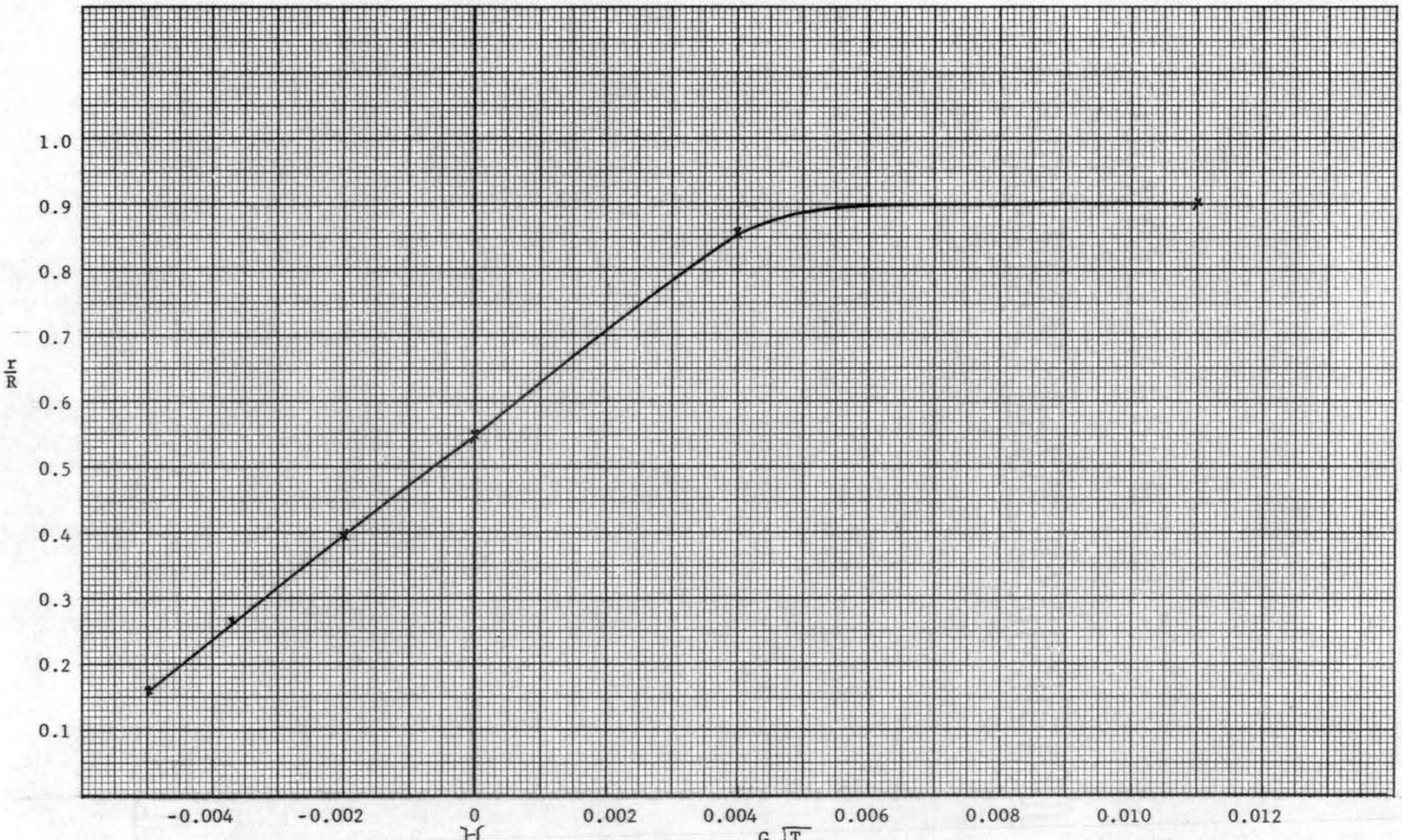

Figure 8. Calculated mass-bleed rate, $\mathcal{H} = 1.088 \frac{G_d\sqrt{T_o}}{P_o A_b}$, versus effective pumping radius ratio r/R, for conical jet mixing, $M_1 = 2$

CHAPTER V

CONCLUSIONS AND RECOMMENDATIONS

Beheim (3) concluded that the portion of the cone surface with radius ratio about $r/R > 0.5$ is actually effective for jet pumping. This value of $r/R = 0.5$ satisfactorily agress with Zumwalt's steady, non-bleed axi-symmetric solution for $M = 2$. However, this value becomes invalid for mass-bleed cases.

In this paper, basing on Zumwalt's conical wake flow model, Tang's modification for mass bleeding and Sandia's experimental data, the final conclusion achieved is that the effective pumping surface radius linearly varies with the amount of mass. This result has been shown in Equation (8) and plotted in Figure 8. An equation was derived for the linear portion of the curve: $r/R = 0.55 + 77.5\,\mathcal{H}$.

The validity of Equation (8) for Mach numbers other than two is still questionable. Therefore it is suggested that more experiments be performed to determine the interaction between effective pumping surface and mass bleeding under there conditions. In fact, the Mach number varies rapidly under transient flow condition, such as the case where blast waves pass a re-entry missile. Thus, more experiments for different Mach numbers are duly required to obtain more necessary information in the exploritation of this field.

SELECTED BIBLIOGRAPHY

1. Korst, H. H., Page, R. H., and Childs, M. E. A Theory for Base Pressures in Transonic and Supersonic Flow. Univ. of Illinois, ME-TN-392-2, OSR-TN-55-89, Contract No. AF 18(600)392, March 1955.

2. Zumwalt, G. W. Analytical and Experimental Study of the Axially-Symmetric Supersonic Base Pressure Problem. Ph.D, Dissertation, Univ. of Illinois, 1959.

3. Beheim, M. A. Flow in the Base Region of Axisymmetric and Two-Dimensional Configurations. Lewis Research Center, NASA-TR-R-77, 1960.

4. Korst, H. H., Page, R. H., and Childs, M. E. Compressible Two-Dimensional Jet Mixing at Constant Pressure. Univ. of Illinois, ME-TN-392-1, OSR-TN-54-82, Contract No. AF 18(600)392, April, 1954.

5. Love, E. S. Base Pressure at Supersonic Speeds on Two-Dimensional Airfoils and on Bodies of Revolution with and Without Fins Having Turbulent Boundary Layers. NACA TN-3819 Report, January 1957.

6. Zumwalt, G. W. and Tang, H. H. Computation Curves for Axi-Symmetric Base Pressure Analysis. Research Report Prepared for the Aero-Thermodynamics Dept. of Sandia Corporation, Albuquerque, N.M., by the Office of Engineering Research, Okla. State Univ., Stillwater, Okla. Rpt. No. SBW-4, April 1963.

7. Tripp, Wilson. Analytical and Experimental Investigation of the Base Pressure Behind a Blunt Trailing Edge for Supersonic Two-Dimensional Flow. (Approaching streams have same stagnation temperatures, but different Mach numbers and stagnation pressures). Ph.D. Thesis, Univ. of Illinois. June 1956.

8. Maydew, R. C., and Reed, J. F. Turbulent Mixing of Axi-symmetric Compressible Jets (In the Half-Jet Region) with Quiescent Air. SC-4764(RR). Sandia Corporation, Albuquerque, N.M., March 1963.

9. Chrisman, C. C., and Zumwlat, G. W. Evaluation of the Free Jet Spreading Rate Parameter for Axi-Symmetric Air Flow at M = 3. Research Report Prepared for the Aero-Thermodynamics Dept. of Sandia Corporation, Albuquerque, N.M., by the Office of Engineering Research, Okla. State Univ., Stillwater, Oklahoma. Rpt. No. SBW-3, June 1962.

10. Tang. H. H. and Zumwalt, G. W. Adaptation of Chapman's Laminar Jet Mixing Theory for Use in Non-Stready Base Pressure Problems. Research Report Prepared for the Aero-Thermodynamics Dept. of Sandia Corporation, Albuquerque, N.M., by the Office of Engineering Research, Okla. State Univ., Stillwater, Okla. Rpt. No. SBW-2, June 1962.

11. Tang. H. H. Analytical and Experimental Study of Blast Wave Interaction with the Base Region of an Axially Symmetric Supersonic Missile. Ph.D. Dissertation, Oklahoma State University, 1963.

12. Binder, R. C. Fluid Mechanics, Prentice Hall, Inc.

13. Zumwalt, G. W. and Tang, H. H. Blast Wave Effect on Missile Base Pressure. Research Report Prepared for the Aero-Thermodynamics Dept. of Sandia Corporation, Albuquerque, N.M., by the Office of Engineering Research, Okla. State Univ., Stillwater, Okla., Rpt. No. SBW-1, June 1961.

14. Chapman, D.R. An Analysis of Base Pressure at Supersonic Velocities and Comparison with Experiments. NACA Report 1051, 1951.

15. Reller, J. O., Jr. and Hamaker, F. M. An Experimental Investigation of the Base Pressure Characteristics of Non-Lifting Bodies of Revolution at Mach Numbers from 2.73 to 4.98. NACA TN 3393, March 1955. (Supercedes RM A 52E20)

16. Sivier, K. R. and Bogdonoff, S. M., The Effect of Support Interference on the Base Pressure of a Body of Revolution, Report No. 332, Princeton University, October 1955. (AFOSR TN-55-301)

VITA

WAYNE JOHN YOUNG

Candidate for the Degree of

Master of Science

Thesis: DETERMINATION OF THE EFFECTIVE JET PUMPING SURFACE FOR CONICAL SEPARATED SUPERSONIC FLOW

Major Field: Mechanical Engineering

Biographical:

Personal Data: Born in Mukden, Manchuria, China, November 18, 1930, the son of Tso-Chün Chang and Tzu-Hsin Young.

Education: Graduated from Chien-Kuo High School, Taipei, Taiwan, China, June 1951. Entered Taiwan Provincial Cheng-Kung University, Tainan, Taiwan in August 1951, and received the Bachelor of Science Degree in Mechanical Engineering in June 1955. Entered Oklahoma State University in February 1962 and completed requirements for Master of Science degree in Mechanical Engineering in June 1963.

Professional Experience: Served as Second Lieutenant in Chinese Army from 1955 to 1956. Employed as Junior Construction Inspector at U. S. Army Engineering District, Okinawa Taiwan Area Office from 1956 to 1959. Employed at Taiwan Highway Bureau as Junior Mechanical Engineer from 1959 to 1961. Worked as Research Assistant at Oklahoma State University in 1963.